Figure 2 | Response of the sedimentary system to climate and tectonic perturbations. a, Sediment flux from catchment for a twofold increase (solid line) and decrease (dashed line) in precipitation. **b**,**c**, Grain size distribution (GSD) within fan for models in **a**. Solid line shows 20 mm grain size; dashes indicate 1 Myr intervals; insets show vertical grain size profiles 5 km from apex. **d**, D_{50} released from catchment if a twofold precipitation increase is coupled to exported sediment grain size. **e**, Fan GSD for model **d**. **f**, Sediment flux from catchment for a twofold increase (solid line) and decrease (dashed line) in uplift. **g**,**h**, Fan GSD for models in **f**. **i**, D_{84} released from catchment if uplift increase drives coarse sediment export. **j**, Fan GSD for model **i**. Initial conditions: precipitation, 1 m^2 yr^{-1}; uplift rate, 1 mm yr^{-1}; D_{50}, 40 mm; D_{84}, 70 mm.

steady-state condition with a longer response time of about 1 Myr (Fig. 2a). The decreased sediment flux in response to the change in precipitation promotes a backstepping of the fan toe, reducing the length of the fan. This reduction in system length is accompanied by an increase in the rate of down-system fining[2,16], whereby the coarser fraction of the supplied material is deposited a kilometre closer to the apex (Fig. 2c).

An increase in precipitation will increase the sediment grain size exported from the catchment because channel bed grain size scales with basal shear stress[17]. To relate median grain size,

D_{50}, to the change in rainfall, α, we use existing derivations that combine Manning's equation with boundary shear stress to link grain size to catchment water discharge[18]. Assuming that water flux is directly proportional to rainfall within the catchment, $D_{50} \propto \alpha^{3/5}$. Increased erosion in the catchment acts to reduce channel slope until topographic steady state is attained. Input granulometry responds on a similar timescale to sediment flux[19], so the grain size distribution returns to the initial condition at a decay half-time of 1 Myr (Fig. 2d). The response recorded within the basin to a coupled increase in precipitation and sediment calibre is a marked progradation (of order 10 km) of coarse material down-system (Fig. 2e).

Following a perturbation in fault slip rate, the response time for the catchment to reach a new steady state is of the order of 1 Myr (Fig. 2f). An increase in fault slip rate from 1 to 2 mm yr^{-1} generates an increase in sediment flux as erosion within the catchment works to remove the additional mass of rock. A change in subsidence rate within the basin is instantaneous, whereas catchment erosion takes time to respond. Consequently, the amount of material eroded is initially less than the new steady state (Fig. 2f). Fan length is initially short and down-system rate of grain size fining high during this period of transient response[2,5,15]. Down-system grain size trends then return to the same values observed before the perturbation (Fig. 2g). The transient response to an increase in fault slip rate is recorded within the stratigraphy as a small (about 1 km) backstepping of the fan toe and a grain size reduction (Fig. 2g). In contrast, a reduction in fault slip rate causes a progradation of a thin wedge of coarse material into the basin, transporting larger grains (>20 mm) up to a kilometre further down-system (Fig. 2h). The response to a fault slip rate reduction is similar to that of an increase in precipitation, but the grain size signal does not travel down the full length of the system (Fig. 2e,h).

Field data from the central Apennines of Italy have shown that larger clasts are typically exported from fault-bounded catchments following an increase in fault slip rate[19]. For a doubling of slip rate, median grain size of the supply remains relatively unchanged, whereas the coarse end increases from a D_{84} of 70 to 100 mm (ref. 19; Fig. 2i). The increase in D_{84} is transient as increased erosion lowers topographic slopes, before returning to the initial steady-state values over a decay half-time of 1 Myr (ref. 19). The response of the depositional system to an increase in the ratio D_{84}/D_{50} in the sediment released is to accentuate the abrupt backstepping of the fan toe and to promote a more rapid rate of grain size fining (Fig. 2j). The increase in D_{84}/D_{50} increases the rate of selective deposition, as larger grains are preferentially extracted up-system[2].

The deposition of conglomeratic sheets down-system has been previously linked to increases in precipitation in the upstream catchment[20]. For example, a 10-m-thick coarse gravel unit in the 0.6–3-Myr-old St David Formation in the San Pedro Valley of southern Arizona was deposited during a period of tectonic quiescence[21]. Similarly, the Palaeocene–Eocene boundary in the Tremp basin of the Spanish Pyrenees coincides with the presence of a conglomerate sheet that is about 10 m thick, bounded above and below by different palaeosols that indicate an increase in precipitation rate[22]. Sheet conglomerates can be formed from a sharp reduction in subsidence (Fig. 2h). However, the grain size increase is not as pronounced and the progradation is less extensive than that produced by a precipitation increase (Fig. 2b,e). Increased precipitation[23] and unforced internal dynamics[24] may lead to fan-head entrenchment, which may transiently lead to down-system extension of the fan, but this cannot be captured by our time-integrated model. These arguments indicate that thin, laterally extensive gravel sheets within sedimentary basins are best explained by a long-term change in precipitation in upstream catchments.

The Fucino basin, central Italy, is a recently drained lake containing fluvial–deltaic deposits that prograded into the basin from the northwest–southeast boundary faults from the late

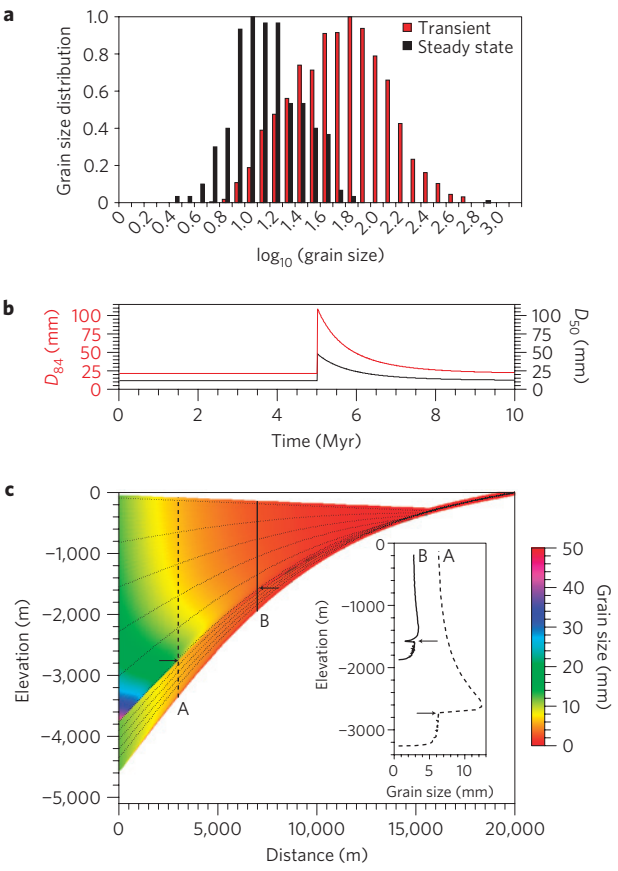

Figure 3 | Predicted response to a fivefold increase in uplift within the Gole di Celano and the Fucino basin system. a, Normalized Wolman point count grain size measurements from the Gole di Celano for regions that are responding (transient) to a slip rate increase from 0.3 to 1.5 mm yr^{-1} and those that have yet to respond (steady state)[19]. The grain size has been converted to a $\log_{10}$ scale so that the two distributions are Gaussian. **b**, Response of input grain size (D_{50} and D_{84}) due to the change in slip rate. **c**, Grain size distribution for a ×5 increase in slip rate. Inset: Vertical grain size profiles. Small arrows mark the slip rate perturbation recorded within the granulometry.

Pliocene onwards[25]. The Fucino fault experienced an increase in slip rate from 0.3 to 1.5 mm yr^{-1} due to fault linkage at 800 kyr BP (refs 9,26). This was accompanied by an increase in both the median (D_{50} = 11–50 mm) and coarse (D_{84} = 20–110 mm) grain size percentiles exported from the Gole di Celano that cross-cuts the fault (Fig. 3a,b).

The response to a fivefold increase in fault slip rate is complex. From our modelling of the response to slip rate perturbations, a backstepping of coarse material would be predicted. However, the coupling between catchment and fan is not straightforward in this field-calibrated scenario. The increase in D_{50} and D_{84} has different effects on the downstream fining. The increase in median grain size leaving the catchment increases the size of gravel entering the fan. Therefore, the increase in slip rate, resulting in a larger input median grain size, produces a wedge of coarse material that extends into the basin (Fig. 3c). Concomitantly, the larger D_{84}/D_{50} ratio promotes an increase in the rate of down-system grain size fining. At ≤5 km from the fan apex, the sediment grain size increases with time owing to the slip rate perturbation, whereas at distances ≥5 km a reduction is recorded (Fig. 3c). The progradation of coarse gravel predicted close to the fault and observed within the fan deposits from the Celano and neighbouring areas entering the Fucino basin[19,25] does not correspond to an increase in fan length, or a sudden increase in

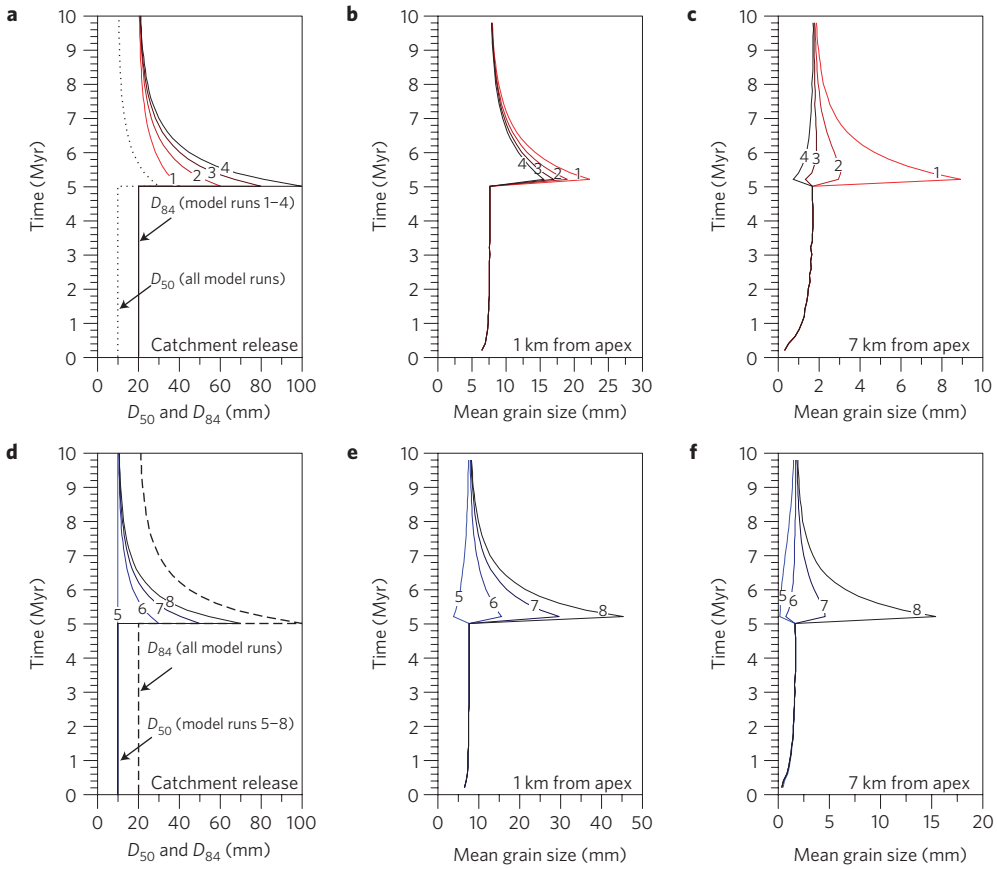

Figure 4 | Down-system grain size signals following a doubling of subsidence and uplift from 1 mm yr^{-1} to 2 mm yr^{-1}. a, Input sediment distributions: dotted line—D_{50}, red to black lines—D_{84} of peak of 40–100 mm. **b**,**c**, Mean grain size deposited plotted in vertical sediment columns 1 and 7 km from the fan apex. Red to black lines are as in **a** and represent the variation in input D_{84}. **d**, Input sediment distributions: dashed line—D_{84}, blue to black lines D_{50} of a peak of 20–70 mm. **e**,**f**, Mean grain size deposited in vertical sediment columns 1 and 7 km from the fan apex. Blue to black lines are as in **d** and represent the variation in input D_{50}.

sediment flux; instead they are a stratigraphic record of the transient response of the eroding landscape.

Sequence stratigraphy is built on an expectation that the lap-out relationships of strata packages are diagnostic of forcing mechanisms and that along time-lines, trends of shallowing (progradation) or deepening (backstepping) are spatially consistent. Our model of a catchment–fan system indicates that stratigraphic grain size and geometries respond in a more complex way to changes in forcing mechanisms. A temporal increase in grain size and onlap of gravel may be recorded close to the fan apex, whereas a reduction in grain size and backstepping of gravel are recorded far from the fan apex (Fig. 4). This downstream change in signal across a stratal package can be described as a transformation in phase, from a positive increase to negative decrease in grain size. There is evidently a trade-off between increased fining due to increased D_{84} of the sediment supply and backstepping of fan architecture, and progradation of large grains due to increased D_{50}. As D_{84}/D_{50} gets larger (>4:1), this phase shift gets larger (Fig. 4).

The terrestrial sedimentary archive is intimately linked to the eroding landscape, but these connections are not linear[6,11]. By combining field observations with a clear physical model of landscape erosion and deposition, we have demonstrated how the response of landscapes to long-term changes in climate and tectonics is recorded and transformed in sedimentary strata. Grain size characteristics released from a catchment impose a strong, but not necessarily linear, control on the stratigraphic record of downstream grain size fining. In illustrating how climatic and tectonic signals are transformed from source region to stratigraphic end-product, and how they may be discriminated from each other, this contribution provides improved concepts for the inversion of the sedimentary record for past changes in external forcing mechanisms.

Methods

Below we provide a brief summary of the methods; further information is provided in the Supplementary Information. We target a relatively simple sediment routing system comprising a small 10-km-long frontal catchment and <20-km-long alluvial fan, separated by a vertical normal fault (Fig. 1). Erosion and deposition are considered along the centre of the catchment and fan[6,15] (Fig. 1). Simplifying the sedimentary system to a two-dimensional plane can be justified as long as there is no long-term flux of sediment in and out of the plane. This can be safely assumed if the mountain front has a series of transverse catchment–fans that are not interconnected, and where over time, any along-strike inequalities in sediment deposition are evened out by channel and fan segment switching in response to differential topographic gradients. The uplifted catchment is eroded, supplying a sediment discharge that is deposited within the basin. Erosion is of the form of a diffusive–concentrative equation[13],

$$\frac{\partial h}{\partial t} = -\frac{\partial q_s}{\partial x} + U(x,t) = \frac{\partial}{\partial x}\left(\kappa + c(\alpha x)^n\right)\frac{\partial h}{\partial x} + U(x,t) \qquad (1)$$

The sediment flux, q_s, is split into hillslope diffusion, $\kappa(\partial h/\partial x)$, and fluvial diffusion, $c(\alpha x)^n(\partial h/\partial x)$, assuming that fluvial processes are proportional to precipitation. In equation (1), h is elevation, x is down-system distance, $\kappa = 0.01$ m^2 yr^{-1} is the linear diffusivity, $c = 1\times10^{-6}$ (m^2 yr^{-1})$^{1-n}$ is the nonlinear sediment transport coefficient, α is the precipitation rate and $n = 2$ is the exponent that describes the dependency of sediment discharge on fluid transport[14,15]. $U(x,t)$ is the uplift within the catchment, which can be varied as the system evolves. Equation (1) is made dimensionless by the length of the catchment, $l_x = 10$ km, and the timescale l_x^2/κ, giving

$$h = l_x\tilde{h} \qquad x = l_x\tilde{x} \qquad t = \frac{l_x^2}{\kappa}\tilde{t}$$

Equation (1) therefore becomes,

$$\frac{\partial \tilde{h}}{\partial \tilde{t}} = \frac{\partial}{\partial \tilde{x}}\left(1 + D_e \tilde{x}^n\right)\frac{\partial \tilde{h}}{\partial \tilde{x}} + \tilde{U} \qquad (2)$$

where $\tilde{U}$ is the dimensionless uplift and D_e expresses the relative importance of concentrative processes versus diffusive processes,

$$D_e = \frac{c\,(\alpha l_x)^n}{\kappa}$$

The uplift field is that of fault-bounded blocks[27]. Equation (2) is solved using a standard finite-element approach with linear weighting functions and linear time-steps[28]. Sediment flux, q_s, is sensitive to the boundary condition at the catchment outlet, which we refer to as the apex boundary condition (Fig. 1).

Depositional architecture is calculated by a volume balance approach, assuming that no erosion occurs within the depositional fan[14]. In our model the absolute elevation of the apex boundary condition is free to move, but we impose continuity of gradient at the apex boundary condition, as observed in natural catchment–fan systems[29]. We then iterate to determine the gradient of the fan surface that equals the gradient of the catchment outlet surface that balances the volume of sediment released[15]. The slope of the fan is assumed to be constant. Therefore, at each time increment, the new depositional wedge is determined, and selective deposition theory is used to estimate down-system grain size fining in the stratigraphy. By treating fan deposition as a simple balance of sediment budget with accommodation space provided, we time integrate the individual processes such as changes in fan width within single channel flows. Therefore, whereas at the timescale of single flood events the depositional geometry and downstream fining may be representative of the sediment hydrodynamics of the active layer, at the long timescales considered here the depositional geometry and downstream fining in stratigraphy can be approximated by our volume balance approach.

The initial grain size signal is transformed down-system by selective deposition using an adapted version of self-similar solutions for down-system grain size trends[2,16]. The self-similar solutions assume a normal distribution of sediment grain size. We therefore convert the grain size distribution to a logarithmic scale and sort by the diagnostic standard deviation, ϕ_0, and mean, $\tilde{D}_0$ (see Supplementary Information). Down-system fining is then governed by the following set of equations[16],

$$\tilde{D}(x^*) = \tilde{D}_0 + \phi_0 \frac{1}{C_v}\left(e^{-C_l y^*} - 1\right)$$

where $x^* = x/l_f$ and $l_f = 20$ km is the length of the basin, $C_l = 0.7$ (ref. 2), $C_v = 0.25$ (see Supplementary Information) and y^* is a spatial transformation of x^*. This is given by[30],

$$\frac{dy^*}{dx^*} = R^*$$

R^* is the distribution of deposition given by

$$R^* = \left(1 - \lambda_p\right)\frac{S(x^*)}{q_s(x^*)}$$

where $\lambda_p = 0.3$ is the sediment porosity, $S(x^*)$ is the dimensionless area of accommodation space generated at a given time step and $q_s(x^*)$ is the equivalent down-system distribution of sediment flux.

Received 26 October 2010; accepted 21 January 2011; published online 27 February 2011

References

1. Zhang, P. Z., Molnar, P. & Downs, W. R. Increased sedimentation rates and grain sizes 2–4 Myr ago due to the influence of climate change on erosion rates. *Nature* **410,** 891–897 (2001).
2. Duller, R. A. *et al.* From grain size to tectonics. *J. Geophys. Res.* **115,** F03022 (2010).
3. Flemings, P. B. & Jordan, T. E. A synthetic stratigraphic model of Foreland basin development. *J. Geophys. Res.* **94,** 3851–3866 (1989).
4. Paola, C., Heller, P. & Angevine, C. The large-scale dynamics of grainsize variation in alluvial basins: 1. Theory. *Basin Res.* **4,** 73–90 (1992).
5. Braun, J. in *Anologue and Numerical Modelling of Crustal-Scale Processes* Vol. 253 (eds Buiter, S. J. H. & Schreurs, G.) 307–325 (Geological Society, Special Publications, 2006).
6. Humphrey, N. F. & Heller, P. L. Natural oscillations in coupled geomorphic systems—an alternative origin for cyclic sedimentation. *Geology* **23,** 499–502 (1995).
7. Clevis, Q., d Boer, P. & Wachter, M. Numerical modelling of drainage basin evolution and three-dimensional alluvial fan stratigraphy. *Sedim. Geol.* **163,** 85–110 (2003).
8. Montgomery, D. R. & Stolar, D. B. Reconsidering Himalayan river anticlines. *Geomorphology* **82,** 4–15 (2006).
9. Whittaker, A. C. *et al.* Contrasting transient and steady-state rivers crossing active normal faults: New field observations from the Central Apennines, Italy. *Basin Res.* **19,** 529–556 (2007).
10. Cowie, P. A. *et al.* New constraints on sediment-flux-dependent river incision: Implications for extracting tectonic signals from river profiles. *Geology* **36,** 535–538 (2008).
11. Allen, P. A. in *Landscape Evolution: Denudation, Climate and Tectonics Over Different Time and Space Scales* Vol. 269 (eds Gallacher, K., Jones, K. S. J. & Wainwright, J.) 7–28 (Geological Society, Special Publications, 2008).
12. Horton, B. K., Constenius, K. N. & DeCelles, P. G. Tectonic control on coarse grained foreland-basin sequences: An example from the Cordilleran foreland basin, Utah. *Geology* **32,** 637–640 (2004).
13. Smith, T. R. & Bretherton, F. Stability and conservation of mass in drainage basin evolution. *Wat. Resour. Res.* **8,** 1506–1529 (1972).
14. Simpson, G. & Schlunegger, F. Topographic evolution and morphology of surfaces evolving in response to coupled fluvial and hillslope sediment transport. *J. Geophys. Res.* **108,** B62300 (2003).
15. Densmore, A. L., Allen, P. A. & Simpson, G. Development and response of a coupled catchment fan system under changing tectonic and climatic forcing. *J. Geophys. Res.* **112,** F01002 (2007).
16. Fedele, J. J. & Paola, C. Similarity solutions for fluvial sediment fining by selective deposition. *J. Geophys. Res.* **112,** F02038 (2007).
17. Wiberg, P. L. & Smith, J. D. Calculations of the critical shear–stress for motion of uniform and heterogeneous sediments. *Wat. Resour. Res.* **23,** 1471–1480 (1987).
18. Attal, M. *et al.* Modelling fluvial incision and transient landscape evolution: Influence of dynamic channel adjustment. *J. Geophys. Res.* **113,** F03013 (2008).
19. Whittaker, A. C., Attal, M. & Allen, P. A. Characterising the origin, nature and fate of sediment exported from catchments perturbed by active tectonics. *Basin Res.* **22,** 809–828 (2010).
20. Heller, P. L. & Paola, C. The large-scale dynamics of grain size variation in alluvial basins, 2: Application to syntectonic conglomerate. *Basin Res.* **4,** 91–102 (1992).
21. Lindsay, E. H. *et al.* Sediments, geomorphology, magnetostratigraphy and vertebrate paleontology in the San Pedro Valley, Arizona. *J. Geol.* **98,** 605–619 (1990).
22. Schmitz, B. & Pujalte, V. Abrupt increase in seasonal extreme precipitation at the Paleocene–Eocene boundary. *Geology* **35,** 215–218 (2007).
23. Dühnforth, M. *et al.* Controls on sediment evacuation from glacially modified and unmodified catchments in the eastern Sierra Nevada, California. *Earth Surf. Proc. Land.* **33,** 1602–1613 (2008).
24. Pepin, E., Carretier, S. & Herail, G. Erosion dynamics modelling in a coupled catchment–fan system with constant external forcing. *Geomorphology* **122,** 78–90 (2010).
25. Cavinato, G. P. *et al.* Sedimentary and tectonic evolution of Plio-Pleistocene alluvial and lacustrine deposits of Fucino Basin (central Italy). *Sedim. Geol.* **148,** 29–59 (2002).
26. Roberts, G. P. *et al.* Fault scaling relationships, deformation rates and seismic hazards: An example from the Lazio-Abruzzo Apennines, central Italy. *J. Struct. Geol.* **26,** 377–398 (2004).
27. Anders, M. H. *et al.* The growth of fault-bounded tilt blocks. *Tectonics* **12,** 1451–1459 (1993).
28. Zienkiewicz, O. C. & Taylor, R. L. *The Finite Element Method* Vol. 1. (Butterworth-Heinemann, 2000).
29. Bull, W. B. *Geomorphology of Segmented Alluvial Fans in Western Fresno County, California* (Prof. Paper, US Geological Survey, 1964).
30. Paola, C. & Seal, R. Grain size patchiness as a cause of selective deposition and downstream fining. *Wat. Resour. Res.* **31,** 1395–1407 (1995).

Acknowledgements

The numerical model was developed through collaborations with G. Simpson (Université de Geneve) and A. Densmore (University of Durham), and with the help of H.M. Nick (Utrecht University). We would also like to thank H. M. Bjornseth and I. Lunt (Statoil) for their constructive input on this work. This work was funded by Statoil through a generic research programme on sediment routing systems.

Author contributions

J.J.A. designed and carried out the numerical experiments. All authors contributed equally to the analysis of the results and writing of the manuscript.

Additional information

The authors declare no competing financial interests. Supplementary information accompanies this paper on www.nature.com/naturegeoscience. Reprints and permissions information is available online at http://npg.nature.com/reprintsandpermissions. Correspondence and requests for materials should be addressed to J.J.A